

Slip Ratio for Lugged Wheel of Planetary Rover in Deformable Soil: Definition and Estimation

Liang Ding, Haibo Gao, Zongquan Deng, Kazuya Yoshida, and Keiji Nagatani

Abstract—The wheel slip ratio is an important state variable in terramechanics research and the control of planetary rovers. Definitions of the slip ratio for a wheel with lugs and methods of estimating it for all wheels onboard have seldom been attempted. This paper presents several definitions for the slip ratio of a lugged wheel, which can be interconverted by altering the shearing radius. Equations for calculating the longitudinal velocity and slip ratio of a wheel moving on rough terrain are deduced from the horizontal speed of the wheel's axle. Wheel-soil interaction experiments were performed for two types of wheels with different radii and lugs of different heights. The drawbar pull, torque, and wheel sinkage were measured using sensors. These data confirmed the effectiveness of the proposed slip ratio definition methods. Furthermore, two slip ratio estimation methods are proposed and verified: a visual information-based method by analyzing the lug traces marked on the terrain with high precision, and a terramechanics-based method in which the equations for the vertical load and torque are solved to estimate the slip ratios of all wheels.

I. INTRODUCTION

WHEELED mobile robots (rovers) have played and will play significant roles in planetary exploration missions. Successful examples include the Mars rovers (Sojourner, Spirit, and Opportunity) of the USA and the lunar rovers of the former Soviet Union (Lunakhod). Several new rover-based planetary exploration plans have recently been established, such as the Mars Science Laboratory mission, ExoMars mission, and lunar exploration projects. These new missions require the rovers to travel over terrain that is more challenging than has ever been encountered before.

When moving across the challenging deformable terrain of the moon or Mars, a rover is prone to slip, causing it to waste

This work was supported by National High Technology Research and Development Program of China (grant No. 2006AA04Z231), Key Natural Science Foundation of Heilongjiang Province in China (grant No. ZJG0709) and Foundation of Chinese State Key Laboratory of Robotics and Systems (grant No. SKLRS200801A02), and "111" Project (grant No. B07018).

L. Ding, H. Gao, and Z. Deng are with School of Mechatronics Engineering, Harbin Institute of Technology, Harbin 150001, Heilongjiang, China; the State Key Laboratory of Robotics and System (HIT), Harbin 150001, Heilongjiang, China (e-mail: liangding@astro.mech.tohoku.ac.jp, gaohaibo@hit.edu.cn, denzq@hit.edu.cn).

K. Yoshida, K. Nagatani, and L. Ding are with the Department of Aerospace Engineering, Tohoku University, Aoba 6-6-01, Sendai, 980-8579, Japan (e-mail: yoshida@astro.mech.tohoku.ac.jp, keiji@ieee.org).

time and energy, or in the worst case, to even get stuck [1], [2]. Slip is defined as the difference between the theoretical circumference velocity ($r\omega$) and the actual traveling velocity (v) of a wheel or vehicle. The slip ratio is a relative quantity used to express the degree of slip.

The slip ratio is an indispensable variable for research on wheel-soil interaction mechanics (terramechanics), which is of great importance to the design, control, and simulation of a rover. The maximum stress angle [3] and shear displacement of soil [4], which are used to calculate the normal stress and shear stress acting on a wheel by soil, are both functions of the slip ratio. As a result, the slip ratio is usually used as an independent variable for research on the drawbar pull, resistance torque, sinkage, tractive efficiency, etc. of a wheel [5]–[7].

While traveling across a rough deformable planetary terrain, it is useful to estimate the slip ratio of a rover and limit it to under a certain value, in order to decrease slip-sinkage, avoid getting a wheel stuck, and improve tractive efficiency. For example, the Opportunity rover experienced 100% slip, causing it to get stuck in "Purgatory Dune" in April 2005, with a resulting delay of five weeks [2]. That experience caused the rover team to implement slip checks that stop the rover from driving if its slip ratio is beyond a certain amount. After each blind drive segment of several meters (e.g., 5 meters), Visual Odometry would be used to perform a Slip Check for the rover [8]. On Martian solar day (sol) 603, the Opportunity rover was successfully stopped when the onboard slip check reported a slip ratio of 0.445, which was larger than the high limit slip ratio of 0.40 set for the traverse on that sol [8], [9]. Based on a knowledge of terramechanics, a traction control method was developed for targeting a small slip ratio and limiting the driving torque to prevent it from exceeding the maximum shear stress of the soil [1], [10]. This method allowed the rover to successfully traverse deformable terrain with obstacles without digging into the soil or becoming stuck, whereas the velocity control method resulted in a fatal situation. Path following control algorithms that consider slip compensation were also developed in order to avoid the error caused by wheel slip [11]–[13].

It is important to estimate the slip ratio of a rover for onboard application [8]. Several methods have been developed to predict the slip ratio of a rover vehicle based on visual information [14], or in combination with data obtained from an inertial measurement unit (IMU) [12].

For smooth wheels without obvious lugs, the slip ratio can be calculated using the radius of the wheel. However,

planetary rovers usually have wheels with lugs of a certain height to improve the tractive performance [6], [15]. Predicting the slip ratio precisely is based on the premise of defining it reasonably. However, methods for defining the slip ratio of a lugged wheel have seldom been considered in previous research. In order to coordinate the motion of each wheel on rough terrain to decrease energy consumption, it is necessary to estimate the slip ratios of all the wheels in real time. This paper discusses several definition methods for the slip ratios of lugged planetary wheels and their relationships. Two slip ratio estimation methods are presented: a visual information-based method involving high-precision analysis of the lug trace marks left on the terrain, and a terramechanics-based method in which the equations for the vertical load and torque of a single wheel are solved and then used to estimate the slip ratios of all wheels.

This paper is organized as follows. Section II defines the slip ratio for a lugged wheel. Section III presents some wheel-soil interaction experiments. In Sections IV and V, two slip ratio estimation methods are investigated.

II. DEFINITION OF SLIP RATIO FOR LUGGED WHEEL

A. Slip Ratio of Smooth Wheel

For a smooth wheel without lugs, the slip ratio is defined as a function of the longitudinal traveling velocity and the circumference velocity of the wheel:

$$s = \begin{cases} (r\omega - v) / r\omega & (r\omega \geq v, 0 \leq s \leq 1) \\ (r\omega - v) / v & (r\omega < v, -1 \leq s < 0) \end{cases} \quad (1)$$

where r is the radius of the wheel, v is the traveling velocity, ω is the angular velocity, and $r\omega$ is the circumference velocity. If $s > 0$, the wheel slips; if $s = 0$, the wheel rolls without slipping or skidding; and if $s < 0$, the wheel skids, where $|s|$ is actually the skid ratio, reflecting the degree of wheel skid. Generally, a driven wheel slips while climbing up a slope or moving on flat terrain, while a towed wheel or a driven wheel moving down a slope will skid. Fig. 1 shows the velocity distribution and instantaneous center where the velocity is zero for wheels with different slip ratios.

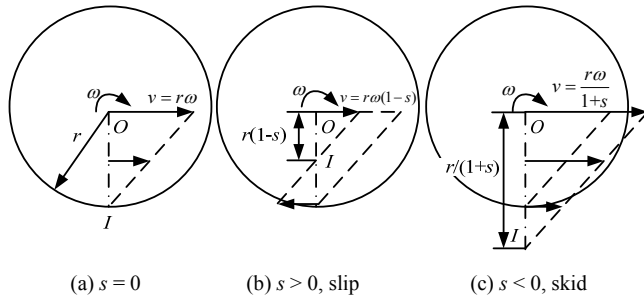


Fig. 1 Velocity and instantaneous center for wheels with different slip ratios.

B. Definition of Slip Ratio for a Lugged Wheel

For a lugged wheel, it is unreasonable to calculate the slip ratio with (1) because the wheel lugs will generate considerable drawbar pull even if the slip ratio is zero. Actually, a wheel moving on smooth terrain should work with a positive slip ratio in order to compensate for the soil

resistance to get a zero drawbar pull. In order to avoid the above contradiction, the definition of slip ratio for a lugged wheel should be considered. The most important problem is determining the shearing radius of the wheel to calculate the slip ratio:

$$r_s = r + \lambda_s h \quad (0 \leq \lambda_s \leq 1) \quad (2)$$

where h is the lug height and λ_s is the lug shearing coefficient. The shearing radius is the average radius where the shearing between moving soil and static soil occurs.

There are several ways to determine λ_s and different slip ratios will be obtained for a certain group of v and ω .

1) s_1 : Let s_1 denote the slip ratio calculated with (1), corresponding to $\lambda_{s1} = 0$.

2) s_2 : If the wheel lugs are relatively high and the space between two lugs is sufficiently small, the lug space can be considered as filled with soil moving together with the wheel. Then the shearing radius is the maximum radius of the wheel, i.e., $\lambda_{s2} = 1$, and (3) is obtained:

$$s_2 = \begin{cases} [(r+h)\omega - v] / [(r+h)\omega] & (r\omega + h\omega \geq v, 0 \leq s \leq 1) \\ [(r+h)\omega - v] / v & (r\omega + h\omega < v, -1 \leq s < 0) \end{cases} \quad (3)$$

For conventional terrestrial vehicle tires with very low lugs, this definition of slip ratio is reasonable and usually used. But it is defective for a planetary rover wheel with high and thin lugs, because the smooth surface of the wheel moves with a negative slip ratio when s_2 is zero and the high lugs can cause extra resistance to the wheel. This means that a large negative drawbar pull will be caused even if the slip ratio is zero, as shown in Fig. 6(a). The actual reason is that the wheel cannot move all of the soil between two lugs as a whole because of the flow of the soil.

3) s_3 : If the slip ratio is zero, the lugs should not cause an obvious drawbar pull or resistance to the wheel. For a smooth wheel with a slip ratio of zero, the soil resistance is small because the wheel sinkage is small and the loose soil cannot generate an obvious resistance force. The experimental results for a wheel without lugs shown in Fig. 6(a) demonstrates this situation. Taking the limitations of both s_1 and s_2 into account, the drawbar pull can be considered as zero if the slip ratio calculated with this shearing radius is zero. The value of λ_{s3} is the increasing function of the internal friction angle of the soil and the number of lugs. If the internal friction angle is large and there are sufficient lugs, making most of the soil between two adjacent lugs move with the wheel, s_3 is close to 1. It can also be estimated based on terramechanical experiments.

4) s_4 : It is not easy to estimate λ_{s3} in order to calculate s_3 based on a theoretical method for a real planetary rover. If λ_{s3} is unknown, it is better to determine a slip ratio s_4 theoretically, rather than s_3 . According to Janosi's formula [4], for a slip ratio of zero, if there are equal displacements in the soil near both ends of a lug, causing equal shear stresses with opposite directions, the lug effect could be mostly counteracted. As seen in Fig. 2,

$$v_{O2} \Delta t = v_{O1} \Delta t, \quad (4)$$

where $v_{O1} = v - r\omega$, $v_{O2} = (r+h)\omega - v$, and $v = r_{s4}\omega(1-s) =$

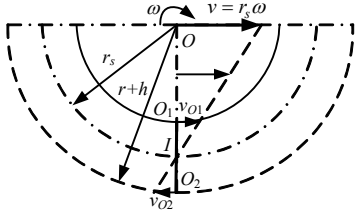


Fig. 2 Velocity distribution for wheel and lugs. $r_{s4}\omega$. It is deduced that:

$$r_{s4} = r + h/2 \quad (5)$$

$$\lambda_{s4} = 1/2 \quad (6)$$

C. Transformation of Different Slip Ratios

Given the value of slip ratio defined by one method, the corresponding slip ratio defined by the other can be calculated. For example, given the slip ratio s' calculated with the shearing radius $r'_s = r + \lambda'_s h$, then the velocity of the wheel is:

$$v = \begin{cases} r'_s \omega (1 - s') & (0 \leq s \leq 1) \\ r'_s \omega / (1 + s') & (-1 \leq s < 0) \end{cases} \quad (7)$$

The slip ratio s calculated with the radius of $r_s = r + \lambda_s h$ is:

$$s = \begin{cases} \frac{r_s \omega - v}{r_s \omega} = 1 - \frac{r'_s}{r_s} (1 - s') = s' + \frac{\lambda_s - \lambda'_s}{r/h + \lambda'_s} (1 - s') \\ \frac{r_s \omega - v}{v} = \frac{r_s}{r'_s} (1 + s') - 1 = s' + \frac{\lambda_s - \lambda'_s}{r/h + \lambda'_s} (1 + s') \end{cases} \quad (8)$$

In the wheel-soil experiments, the slip ratio s_2 was used. Then the slip ratio s_3 was calculated with (9), where λ_{s3} was determined based on the experimental results.

$$s_3 = \begin{cases} s_2 - (1 - \lambda_{s3})(1 - s_2) / (r/h + \lambda_{s3}) \\ s_2 - (1 - \lambda_{s3})(1 + s_2) / (r/h + 1) \end{cases} \quad (9)$$

D. Definition of Slip Ratio for Wheel on Rough Terrain

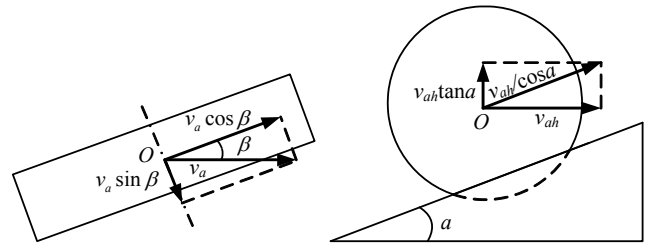
The movement of a wheel on deformable rough terrain can be divided into several situations: climbing up/down a slope, climbing across a slope, or a combination of these. The travelling velocity of the axle of a rover's wheel v_a , especially the horizontal component v_{ah} , can be calculated based on the kinematics information for the rover vehicle as measured by the IMU. But the longitudinal speed of the wheel for calculating the slip ratio cannot be measured directly. Therefore, it is necessary to deduce equations for calculating the wheel's longitudinal velocity based on v_a or v_{ah} .

The angular velocity ω can be measured easily with an encoder. If the longitudinal traveling velocity of wheel v is obtained, the slip ratio can be calculated with (8). The equations for calculating v will be derived.

1) *Velocity for wheel moving with slip angle:* Fig. 3(a) shows a wheel moving on even terrain with slip angle β . The longitudinal velocity of the wheel is:

$$v = v_a \cos \beta \quad (10)$$

2) *Velocity for wheel climbing up/down a slope:* As shown in Fig. 3(b), the wheel velocity while climbing up or down a slope with slope angle α is:



(a) Moving with slip angle
Fig. (3) Basic motion of wheel.

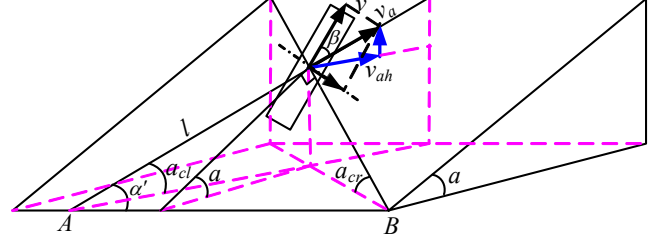


Fig. 4 General circumstances for a wheel moving on a slope.

$$v = v_{ah} / \cos \alpha \quad (11)$$

3) *Velocity for wheel moving on a slope in general circumstances:* Fig. 4 shows the general circumstances of a wheel moving across terrain with slope angle α , where α' is the angle between the moving direction and the horizontal line of the slope. Based on solid geometry, the motion can be divided into two basic motions: climbing up/down the slope with angle α_{cl} and climbing across the slope with angle α_{cr} , where,

$$\alpha_{cl} = \arcsin(\sin \alpha \sin \alpha') \quad (12)$$

$$\alpha_{cr} = \arcsin(\sin \alpha \cos \alpha') \quad (13)$$

Hence, the wheel longitudinal velocity is:

$$v = v_a \cos \beta = \frac{v_{ah} \cos \beta}{\cos \alpha_{cl}} = \frac{v_{ah} \cos \beta}{\sqrt{1 - (\sin \alpha \sin \alpha')^2}} \quad (14)$$

Actually, all of the moving states of the rover can be considered as extreme cases of this general situation. If $\beta = 0$, the wheel moves with no slip angle. If $\alpha = 0$, the wheel moves on a horizontal plane; or it may climb up/down the slope ($\alpha' = 90^\circ$) or climb across the slope ($\alpha' = 0^\circ$).

III. EXPERIMENTAL STUDY OF WHEEL-SOIL INTERACTION

A. Experimental equipment

The wheel-soil interaction testbed developed at Harbin Institute of Technology was used to perform the experiments [16]. It can create various slip ratios by coordinating the velocities of the driving motor and carriage motor. The necessary information, including the wheel sinkage, drawbar pull, vertical load, driving torque, etc., can be measured by relevant sensors with high precision.

B. Experimental Wheels and Planetary Soil Simulant

The experimental wheels were designed based on the current planetary rovers. Two types of cylindrical metal wheels with different radii and widths were used:

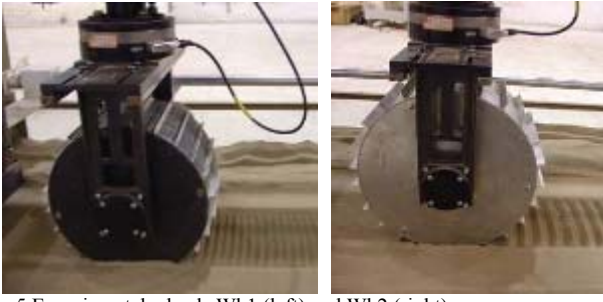


Fig. 5 Experimental wheels Wh1 (left) and Wh2 (right).

$r135 \text{ mm} \times b165 \text{ mm}$ (Wh1), and $r157.35 \text{ mm} \times b165 \text{ mm}$ (Wh2). Wh1 could be equipped with 24 wheel lugs of different heights ($h = 5 \text{ mm}$, 10 mm , and 15 mm) with a space angle of 15° , while Wh2 could be equipped with 30 lugs with a space angle of 12° (Fig. 5). Let n_L denote the number of wheel lugs and $\gamma_L = 2\pi / n_L$ denote the space angle between lugs.

The literature shows that the mechanical properties of dry loose sand are similar to those of planetary soil. Therefore, it is usually used as a planetary soil simulant [6]. The planetary soil simulant used in this study was made from soft sand after removing impurities, sieving, ventilating, and drying. The mechanical parameters were measured using plate-sinkage experiments and shear experiments. The parameters of this soil stimulant are as follows: cohesive modulus of sinkage $k_c = 15.6 \text{ Kpa/m}^{n-1}$, frictional modulus of sinkage $k_\phi = 2407.4 \text{ KPa/m}^n$, sinkage exponent $n = 1.10$, soil cohesion $c = 251 \text{ Pa}$, internal friction angle $\phi = 31.9^\circ$ [17]. Most of these are comparable to those of lunar regolith.

C. Experiment Setup

The experiments showed that the variance of velocity had little impact on the wheel-soil interaction mechanics for a planetary rover's wheel. The traveling velocity of the wheel was set to 10 mm/s . The maximum slip ratio of MER rovers is usually restricted to below 0.4 [9], so that the experimental slip ratios (s_2) are no larger than 0.6 . The vertical load was approximately 80 N , which is comparable to that of the exploration rovers.

D. Results

The wheel interacted with the soil to achieve a steady state after running for several seconds. The steady state data were used to calculate the mean values of sinkage, wheel torque, and drawbar pull after filtering. The data acquisition frequency was 6.67 Hz . As a result, hundreds of pieces of raw data could be obtained during a test. The measured data fluctuated periodically in association with the wheel lugs entering and leaving the soil. In order to verify the repeatability of the experiments, some of them were performed three times. The experimental results showed that the mean values of these repeated experiments were almost the same despite data fluctuation, proving the repeatability and consistency of the experiments [17]. Based on the original data from the experiments, Fig. 6 shows curves for the drawbar pull and torque versus the slip ratio for Wh2. The

values of λ_{s3} for Wh2 with lug heights of 15 mm , 10 mm , and 5 mm were 0.75 , 0.65 , and 0.05 , respectively. Obviously, calculating slip ratio s_3 with λ_{s3} is more reasonable. If $s_3 = 0$, the drawbar pulls of Wh2 with different lugs were all approximately zero and their torques were almost the same, indicating that the wheel lugs had little effect on the wheel-soil interaction mechanics for a zero slip ratio. Fig. 7 compares s_2 , s_3 , and s_4 . The difference between s_3 and s_2 is obvious, while that between s_3 and s_4 is smaller and negligible, verifying the feasibility of substituting s_3 with s_4 for the reason of simplification, although the definition method for s_4 is not very strict because of the flow of sand.

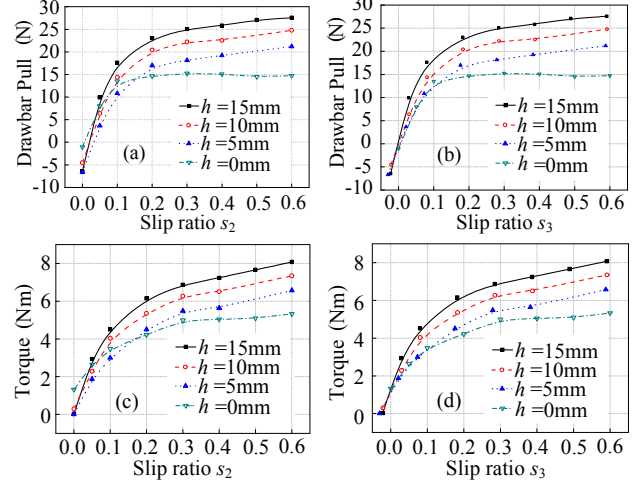


Fig. 6 Experimental torque and drawbar pull versus slip ratio for Wh2.

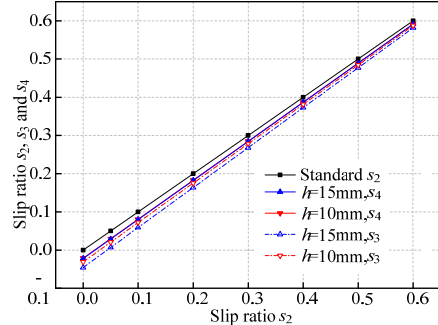


Fig. 7 Comparison of slip ratios calculated with different definition methods.

IV. SLIP RATIO ESTIMATION BASED ON LUG TRACES

As shown in Fig. 8, the stripes of the lug traces became more intensive when the slip ratio was increased. Let T denote the time that a wheel spends in rotating for the angle of γ_L , and L denote the distance between the track prints of two neighboring lugs. According to (3):

$$\hat{s}_2 = \begin{cases} 1 - \frac{vT}{(r+h)\omega T} = 1 - \frac{L}{(r+h)\gamma_L} & (0 \leq \hat{s}_2 \leq 1) \\ \frac{(r+h)\omega T}{vT} - 1 = \frac{(r+h)\gamma_L}{L} - 1 & (-1 \leq \hat{s}_2 < 0) \end{cases} \quad (15)$$

Fig. 9 shows the slip ratio estimation results for the Wh1 wheel with lug heights of 15 mm and 10 mm .

The estimated slip ratios were close to the experimental setting values. The rover can use visual information from cameras for the onboard estimation of slip ratio s_2 , and then s_2

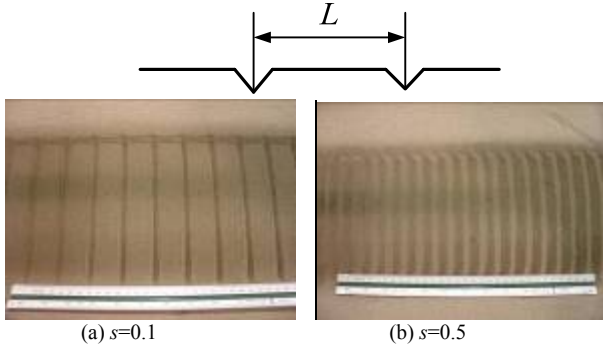


Fig. 8 Lug traces for Wh1 ($h = 10$ mm) with different slip ratios.

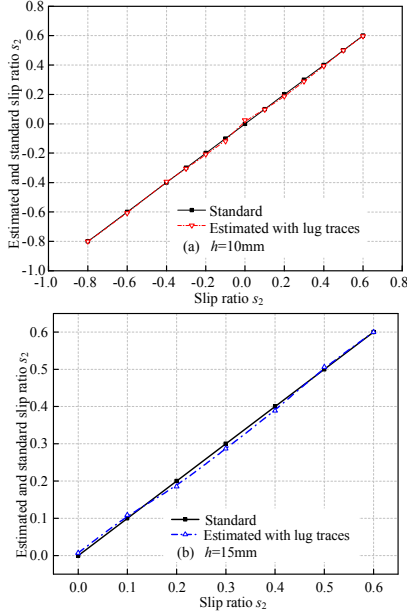


Fig. 9 Slip ratio s_2 estimated with lug traces.

can be used to find s_3 or s_4 with (5). This method is also useful for estimating the slip ratio of an experimental rover in the laboratory by directly measuring the distance between the lug traces. However, this method is infeasible for situations where the slip ratio is too high to generate neat lug traces or the rover has complex motion that destroys the lug traces.

V. TERRAMECHANICS-BASED SLIP RATIO ESTIMATION

A. Wheel-soil interaction mechanics model

Fig. 10 shows a diagram of wheel-soil interaction mechanics [5], where θ_1 is the entrance angle at which the wheel begins to contact the soil, θ_2 is the leaving angle at which the wheel loses contact with the soil, θ_m is the angle of maximum stress, z is the slip sinkage, W is the vertical load of the wheel, DP is the resistance when moving forward, which is equal to the drawbar pull, and T is the driving torque of the motor. The soil interacts with the wheel in the form of continuous normal stress σ and shear stress τ . By improving the Wong-Reece normal stress model [3] and the Janosi shear stress model [4] for the lugged wheel of a planetary rover, equations (16)–(22) were deduced for calculating the stress distributions and concentrated forces/torques. Equation (16)

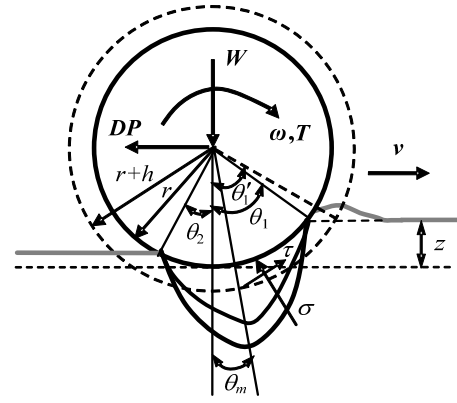


Fig. 10 Wheel-soil interaction mechanics diagram.

can be used to change the constant sinkage exponent with the slip ratio to predict the entire sinkage of the wheel, including the slip sinkage. Equation (17) reflects the lug effect very well by considering the soil deformation θ'_1 . Equation (18) can be used to calculate the leaving angle of the wheel, where c_3 could be made equal to zero for the sake of simplification [5]. Equation (19) is used to calculate θ_m , where $c_1 = 0.5$ and $c_2 = -0.3$. Equations (20)–(22) were improved based on (16)–(19). The parameters c_1 and c_2 can be estimated, while n_0 , n_1 , and k are identified based on the measured data: $n_0 = 0.76$, $n_1 = 1.27$, and $k = 0.012$ m for Wh1, while $n_0 = 0.81$, $n_1 = 1.16$, and $k = 0.011$ m for Wh2. This improved wheel-soil interaction model can predict not only the driving torque and drawbar pull with high precision, but also the wheel sinkage. More details of the model and the parameters can be found in [17].

$$N = n_0 + n_1 s \quad (16)$$

$$\begin{cases} z = r(1 - \cos \theta_1) \\ \theta'_1 = \arccos[(r - z) / R_j] \end{cases} \quad (17)$$

$$\theta_2 = c_3 \theta_1 \quad (18)$$

$$\theta_m = (c_1 + c_2 s) \theta_1 \quad (19)$$

$$\sigma(\theta) = \begin{cases} \left(\frac{k_c}{b} + k_\phi\right) r^N (\cos \theta - \cos \theta_1)^N & (\theta_m \leq \theta \leq \theta_1) \\ \left(\frac{k_c}{b} + k_\phi\right) r^N \left\{ \cos \left[\theta_1 - \frac{\theta - \theta_2}{\theta_m - \theta_2} (\theta_1 - \theta_m) \right] - \cos \theta_1 \right\}^N & (\theta_2 \leq \theta < \theta_m) \end{cases} \quad (20)$$

$$\tau(\theta) = [c + \sigma(\theta) \tan \phi] (1 - e^{-r_s [(\theta'_1 - \theta) - (1-s)(\sin \theta'_1 - \sin \theta)] / k}) \quad (21)$$

$$\begin{cases} W = b \int_{\theta_2}^{\theta_1} [r \sigma(\theta) \cos \theta + r_s \tau(\theta) \sin \theta] d\theta \\ DP = b \int_{\theta_2}^{\theta_1} [r_s \tau(\theta) \cos \theta - r \sigma(\theta) \sin \theta] d\theta \\ T = r_s^2 b \int_{\theta_2}^{\theta_1} \tau(\theta) d\theta \end{cases} \quad (22)$$

B. Estimating slip ratio with the improved model

Given the other parameters, the vertical load W and driving torque T can be considered as functions of θ_1 and slip ratio s :

$$\begin{cases} W = W(\theta_1, s) \\ T = T(\theta_1, s) \end{cases} \quad (23)$$

so that parameters s_1 and θ_1 can be solved as the inverse functions of W and T :

$$\begin{cases} s = s^{-1}(W, T) \\ \theta_1 = \theta_1^{-1}(W, T) \end{cases} \quad (24)$$

It is difficult to derive the explicit form of (24), but it can be solved with a numerical method. The vertical load W and the driving torque T of a rover's wheel could be measured or estimated. W can be computed from a quasi-static force analysis of the rover, and T can be estimated from the electrical current input to the motor [5]. Then, it is possible to estimate the slip ratio s and the entrance angle θ_1 of a lugged wheel by solving (24). The wheel sinkage and drawbar pull can also be predicted with (17) and (22).

Fig. 11 shows a comparison of the estimated slip ratio and standard slip ratio for Wh2. Fig. 12 shows the measured and estimated drawbar pull and wheel sinkage. The error is small, showing the effectiveness of this estimation method.

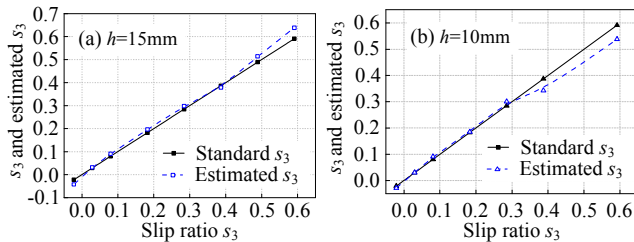


Fig. 11 Slip ratio s_3 estimated with terramechanics model.

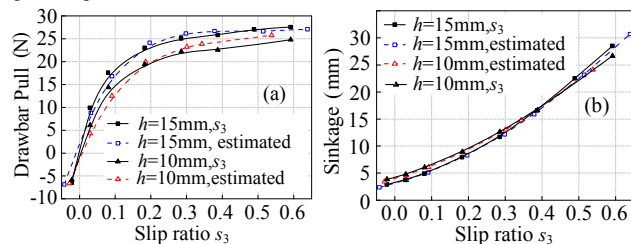


Fig. 12 Comparison of measured and predicted drawbar pull and sinkage.

VI. CONCLUSION

A method for defining the slip ratio of lugged rover wheels has been discussed, including the shearing radius and wheel longitudinal velocity across rough terrain. Experiments showed that the soil can cause little resistance force for a smooth wheel if the slip ratio is zero, because the soil is loose and sinkage is small. Therefore, one important standard for determining the shearing radius is to make the drawbar pull zero for zero slip to eliminate the effect of the wheel lugs. The experimental results for wheels with different lug heights verified this definition method, because the driving torques were also almost the same if the slip ratio was zero. The shearing radius can also be defined as the sum of r and half the lug height h for the sake of simplification. In order to define the slip ratio for a rover on rough terrain, equations were deduced for calculating the longitudinal velocity of a wheel based on the horizontal velocity of the wheel's axle, which can be determined from the kinematics information for the rover vehicle measured by the IMU.

Two slip ratio estimation methods were presented and verified. At low slip, the slip ratio can be estimated by analyzing the lug traces with high precision based on visual

information, which is also helpful for researchers doing experiments with a rover. A more feasible method that can be used for the online estimation of the slip ratios of all the wheels involves solving the equations for the wheel-soil terramechanics. With this method, a slip ratio based control strategy can be realized to save energy, and the motion error of a rover can be compensated for, allowing it to follow the planned path with high precision.

REFERENCES

- [1] K. Yoshida and H. Hamano, "Motion dynamics of a rover with slip-based traction model," in *Proc. of the IEEE Int. Conf. on Robotics & Automation*, Washington, DC, 2002, pp. 3155-3160.
- [2] K. Young (2006, June). Mars rover escapes from the "Bay of Lamentation." Available: <http://space.newscientist.com/article/n9286-ars-rover-escapes-from-the-bay-of-lamentation.html>.
- [3] J. Y. Wong and A. R. Reece, "Prediction of rigid wheel performance based on analysis of soil-wheel stresses, part I: performance of driven rigid wheels," *J. Terramechanics*, vol. 4, no. 1, pp. 81-98, Jan. 1967.
- [4] Z. Janosi and B. Hanamoto, "Analytical determination of drawbar pull as a function of slip for tracked vehicle in deformable soils," in *Proc. of the 1st Int. Conf. of ISTVES*, Torino, Italy, 1961, pp. 707-726.
- [5] H. Shibly, K. Iagnemma, and S. Dubowsky, "An equivalent soil mechanics formulation for rigid wheels in deformable terrain, with application to planetary exploration rovers," *Journal of Terramechanics*, no. 42, pp. 1-13, 2005.
- [6] R. Bauer, W. Leung, and T. Barfoot, "Experimental and simulation results of wheel-soil interaction for planetary rovers," in *Proc. IEEE/RSJ Int. Conf. Intelligent Robots and Systems*, Edmonton, Alberta, Canada, 2005, pp. 586-591.
- [7] G. Ishigami, A. Miwa, K. Nagatani, and K. Yoshida, "Terramechanics based model for steering maneuver of planetary exploration rovers on loose soil," *J. Field Robotics*, vol. 24, no. 3, pp. 233-250, 2007.
- [8] M. Maimone, Y. Cheng and L. Matthies. "Two years of visual odometry on the Mars exploration rovers," *J. Field Robotics*, vol. 24, no. 3, pp. 169-186, 2007.
- [9] Jet Propulsion Laboratory (2005, October 12). NASA Mars exploration rover status 12 October 2005. Available: <http://www.marstoday.com/news/viewsr.html?pid=18352>.
- [10] K. Yoshida, T. Watanabe, N. Mizuno, and G. Ishigami, "Slip, traction control, and navigation of a lunar rover," in *Proc. 6th Int. Symp. on Artif. Intel., Rob. and Auto. in Space*, Nara, Japan, 2003.
- [11] D. M. Helmick, Y. Cheng, D. S. Clouse, et al; "Path following using visual odometry for a Mars rover in high-slip environments," In *Proc. 2004 IEEE Aerospace Conf.*, Big Sky, Montana, 2004, pp.772 - 789.
- [12] D. Helmick, S.I. Roumeliotis, Y. Cheng, D. Clouse, M. Bajracharya, and L. Matthies, "Slip compensation for a Mars rover," in *Proc. 2005 IEEE/RSJ Int. Conf. on Intelligent Robots and Systems*, Edmonton, Canada, 2005, pp. 1419-1426.
- [13] G. Ishigami, K. Nagatani, and K. Yoshida, "Path following control with slip compensation on loose soil for exploration rover," in *Proc. 2006 IEEE/RSJ Int. Conf. on Intelligent Robots and Systems*, Beijing, China, 2006, pp.5552-5557.
- [14] A. Angelova, "Visual prediction of rover slip: learning algorithms and field experiments," Ph.D. dissertation, California Institute of Technology, Pasadena, CA, 2008
- [15] L. Ding, H. Gao, Z. Deng, R. Liu, and P. Gao, "Theoretical analysis and experimental research on wheel lug effect of lunar rover," *Journal of Astronautics*, vol. 30, no. 4, pp. 48-56, 2009.
- [16] L. Ding, K. Yoshida, K. Nagatani, H. Gao, and Z. Deng, "Parameter identification for planetary soil based on decoupled analytical wheel-soil interaction terramechanics model," in *Proc. IEEE/RSJ Int. Conf. Intelligent Robots and Systems*, St. Louis, MO, 2009.
- [17] L. Ding, H. Gao, Z. Deng, K. Yoshida and K. Nagatani, "Wheel-soil interaction mechanics model for planetary rover on loose soil considering lug effect and slip-sinkage," *Journal of ASME Applied Mechanics*, to be submitted for publication.